# Surface tension and nucleation rate of phases of a charged colloidal suspension

Michael Knott* and Ian J. Ford
*Department of Physics and Astronomy, University College London, Gower Street, London WC1E 6BT, United Kingdom*
(Received 16 January 2002; published 7 June 2002)

The square gradient approximation is used to calculate the surface tension between two phases of differing density in a charged colloidal suspension, and the results are compared with experimental and theoretical evidence from various colloidal systems. The nucleation rate of a colloidal liquid cluster from a metastable colloidal gas is estimated using a version of classical nucleation theory. We explain in terms of nucleation phenomena the recently described ''Swiss cheese effect,'' which involves the formation of crystals from an initial disordered state, followed by the formation of disordered regions within the crystals and at the interfaces between them. We argue that this sequence of events shows evidence both of homogeneous and of heterogeneous nucleation. The experimental prominence of homogeneous nucleation suggests that metastability is very important in colloidal systems, and therefore that the consideration of nucleation rates is essential to the study of phase behavior in such systems. We also predict that the occurrence or nonoccurrence of phase separation into a dense and a rarefied phase is governed by the ratio of the macroion charge to the macroion radius.

DOI: 10.1103/PhysRevE.65.061401 PACS number(s): 82.70.Dd, 64.60.Qb, 82.60.Nh, 68.03.Cd

## I. INTRODUCTION

A charged colloidal suspension appears to be an excellent example of the way in which the behavior of a physical system can depend more strongly on generic considerations than on the specific nature of the system. Experimental observations on these systems at low added salt have produced evidence of coexistence between regions of greatly differing macroion density [1–9]. This behavior is strongly reminiscent of the solid- and liquid-gas phase separations that are observed in molecular matter. It occurs in a manner such that it cannot be explained by means of the attractive van der Waals interactions between colloidal particles. Therefore, it can be argued that the phenomenon requires the modification, elaboration, or replacement of the traditional theory [10,11] of colloidal stability, which regards the electrostatic part of the interaction in a charged colloidal suspension as a sum of repulsive effective pairwise interactions between the colloidal particles.

A variety of theoretical approaches have been proposed [12–18] to produce qualitative predictions of phase separation. It appears [15] that the observed coexistence behavior is the result of a competition between the electrostatic component of the free energy, which is cohesive, and the counterion translational entropy, which acts to stabilize the system against phase separation. This interpretation provides a good analogy [16] with the situation in molecular fluids [19], where the cohesive effect is provided by the attractive van der Waals interaction between molecules, while the stabilizing effect is the result of the translational entropy of the molecules. However, neither the theoretical treatments [20] nor the very existence of the phase separation phenomenon [21,22] are universally accepted, although the latter is supported by recent computer simulations [23,24].

Even under conditions where the most thermodynamically favorable state for a system is a mixture of phases, a preexisting homogeneous fluid may persist temporarily. This is because of the free energy barrier associated with the formation of a phase interface: before a large region of the new phase can exist, a small droplet must nucleate, and this droplet will have a large surface area relative to its volume. As a result, the free energy cost of forming the surface of a small droplet outweighs the free energy gain of forming the bulk of the droplet, and the droplet is unstable with respect to the preexisting phase, which we therefore term metastable [25].

In this paper, we apply the principles of nucleation [26] to phase transitions in charged colloidal suspensions. There are a number of reasons for doing this. Experiments by Yoshida *et al*. [8,9] have investigated the evolution of a suspension from an initial homogeneous state to a phase separated final state. It should be possible to explain the resulting ''Swiss cheese'' structure in terms of surface free energies and nucleation; it is clear, then, that the thermodynamic effects of phase boundaries in these systems can be observed and are, therefore, worthy of theoretical investigation. There is also the possibility that insights gained from the consideration of nucleation events in colloidal systems could benefit the study of nucleation processes, in general, and of nucleation processes in molecular systems, in particular. It has often been pointed out that colloidal crystals provide a good model system for atomic matter [27], as similar processes take place at larger length scales and over longer time scales. Nucleation in colloidal systems happens more slowly and on a larger length scale than in molecular systems, where the fast rate of the phase transition and the unobservable size of the critical cluster make the phenomenon very difficult to investigate accurately, either by experiment or by theory. Another problem with the study of homogeneous nucleation in molecular systems is that it may be preempted by heterogeneous nucleation, the process by which the new phase nucleates around foreign bodies or on the walls of the container. The larger length scales in colloidal systems should make heterogeneous nucleation less of a problem: sufficiently large impurities are unlikely to be present in the bulk of a suspension,

*Present address: Department of Biochemistry, Faculty of Medicine, University of Toronto, Toronto, Ontario, Canada M5S 1A8.

 

while the container walls may or may not act as sites for heterogeneous nucleation (depending on whether the free energy of the interface between the nucleating phase and the wall is smaller or larger than that of the interface between the metastable phase and the nucleating phase).

Section II of this paper summarizes a recent theoretical treatment of colloidal phase coexistence by the present authors [16] and introduces an important generalization. In Secs. III–V we use a simple approximate method to calculate the surface tension of an interface in a charged colloidal suspension under conditions of zero added salt. After an introduction to classical nucleation theory and the derivation of the free energy appropriate to the system under consideration (Sec. VI), we investigate the nucleation rate of a liquid cluster from a metastable vapor in a colloidal system (Sec. VII). Finally, we discuss the Swiss cheese effect in the context of nucleation theory in Sec. VIII.

We use SI electromagnetic units throughout.

## II. PHASE COEXISTENCE IN CHARGED COLLOIDAL SUSPENSIONS

We model a system containing a large number $N_M$ of identical spherical colloidal particles (macroions) of radius $a$ and constant surface charge $Ze$, where $e$ is the elementary charge and $|Z| \gg 1$. These are balanced by $N_c = |Z| N_M$ point counterions (microions) of charge $z_c e$, where $|z_c| = 1$. The system contains no added salt. We take the macroions to be negative and the counterions to be positive ($Z < 0$ and $z_c = +1$), but it makes no difference to the results if the signs are interchanged. The solvent in which the ions are suspended has constant temperature $T$ and volume $V$, and is regarded as a continuum of permittivity $\epsilon = \epsilon_r \epsilon_0$, which is unaffected by the presence of ions. Here, $\epsilon_0$ is the permittivity of the vacuum and $\epsilon_r$ is the relative permittivity; we regard the solvent as being water, which has a relative permittivity of around 80.

Correlations between microions are ignored: they respond to a mean field rather than interacting directly with one another. The behavior of the macroions is regarded as adiabatically separated from that of the much smaller counterions; that is, the counterions are allowed to form their equilibrium density profile about a ''fixed'' system of macroions, and then the free energy of the system is found as a function of the macroion density. These simplifications permit the use of a mean field Poisson-Boltzmann description of the counterion distribution. This means that the counterions are modeled as a continuous fluid of charge (of varying density) rather than as a collection of discrete particles.

Since the volume and temperature of the model system are fixed, the appropriate thermodynamic potential to be minimized is the Helmholtz free energy. If we ignore the small contribution from the colloidal particles in the absence of charge, the calculated Helmholtz free energy $f$ per macroion contains [16] two macroion density dependent terms $\Delta f_0$ and $f_{el}$. The first is the macroion density dependent part of the contribution from the counterion ideal gas in the absence of charge, $\Delta f_0 = -|Z| k_B T \ln(v-1)$, where $k_B$ is the Boltzmann constant and $v$ is a dimensionless volume per macroion, in units of the volume $(4/3)\pi a^3$ of one macroion ($v$ is equal to $1/\eta$, where $\eta$ is the colloid volume fraction). The electrostatic contribution $f_{el}$ to the free energy per macroion can be written as a sum of two components $f_{pair}$ and $f_{self}$, where

$$f_{pair} = \frac{Z^2 e^2}{8\pi\epsilon a}\left\{\left[\frac{\sinh\kappa a}{\kappa a} + \frac{\Phi_s}{1+\kappa a}\left(\cosh\kappa a - \frac{\sinh\kappa a}{\kappa a}\right)\right]^2 \Sigma^Y + \frac{4\ln v}{9\pi\kappa^2 a}\sum_{m\neq n}\int_0^\infty I(k)\,dk\,\frac{\sin k a S_{mn}}{k a S_{mn}}\right\} \tag{1}$$

and

$$f_{self} = \frac{Z^2 e^2}{8\pi\epsilon a}\left[\frac{1}{1+\kappa a} + \frac{1}{3}\left(\frac{\kappa a}{1+\kappa a}\right)^2 \Phi_s^2 + \frac{e^{-\kappa a}}{1+\kappa a}\left(\frac{\sinh\kappa a}{\kappa a} - \cosh\kappa a\right)(\Phi_s - 1)^2 - \frac{1}{3}\left(\frac{\kappa a \ln v}{9}\right)^2 + \frac{4\ln v}{9\pi\kappa^2 a}\int_0^\infty I(k)\,dk\right]. \tag{2}$$

Here, $\Phi_s$ is a dimensionless potential at the surface of a macroion in units of $Ze/4\pi\epsilon a(1+\kappa a)$,

$$\Phi_s = \frac{(1+\kappa a)(e^{-\kappa a} + \Sigma^Y)}{(1+\kappa a)e^{-\kappa a} + (1-\kappa a \coth\kappa a)\Sigma^Y}, \tag{3}$$

while $I(k)$ is defined as

$$I(k) = \left\{\left(\frac{7}{2v(ka)^2} - \frac{\ln v}{9}\right)(\sin ka - ka\cos ka)^2 + \sin ka(\sin ka - ka\cos ka)\right\}\left[\ln\left(1 + \frac{\kappa^2}{k^2}\right) - \frac{\kappa^2}{k^2}\right]. \tag{4}$$

$\Sigma^Y$ is a sum over Yukawa potentials, defined by $\Sigma^Y = \Sigma_{n\neq m} e^{-\kappa a S_{mn}}/S_{mn}$, where $S_{mn}$ is a dimensionless separation between macroions $m$ and $n$ in units of $a$. The parameter $\kappa$ is the inverse Debye screening length, defined by $\kappa^2 = z_c^2 e^2 \overline{n_c}/\epsilon k_B T$, where $\overline{n_c}$ is the mean counterion density in the suspension. Each region of the system should be charge neutral, so $\kappa a$ varies, through its dependence on $\overline{n_c}$, as a function of the dimensionless volume $v$,

$$\kappa a = \left(\frac{3|Z|e^2}{4\pi\epsilon k_B T a}\,\frac{1}{v-1}\right)^{1/2}. \tag{5}$$

If a face centered cubic structure is used, the relation between $v$ and the dimensionless nearest neighbor macroion separation $S$ (in units of $a$) is $S = (4\sqrt{2}\pi v/3)^{1/3}$.

The ideal gas term $\Delta f_0$ decreases monotonically with increasing $v$, while $f_{el}$ increases [16]. The graph of $f = \Delta f_0 + f_{el}$ as a function of $v$ may contain an upward bulge (where the second derivative is negative); as in a molecular fluid,

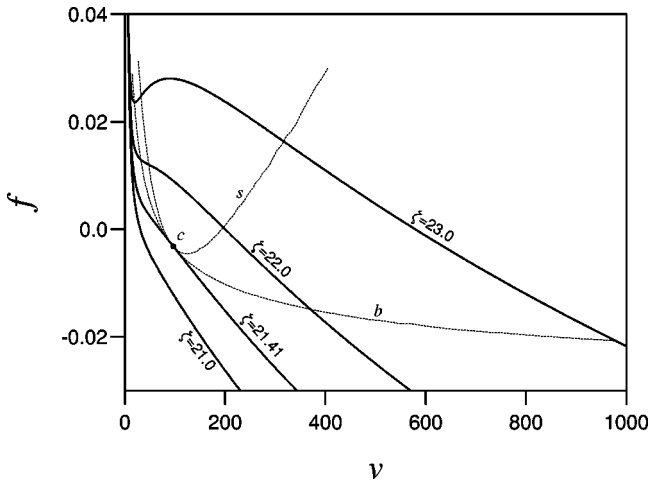


FIG. 1. The free energy $f$ per macroion in units of $Z^2e^2/8\pi\epsilon a$ for various values of $\zeta$. The binodal is marked $b$, the spinodal $s$, and the critical point $c$.

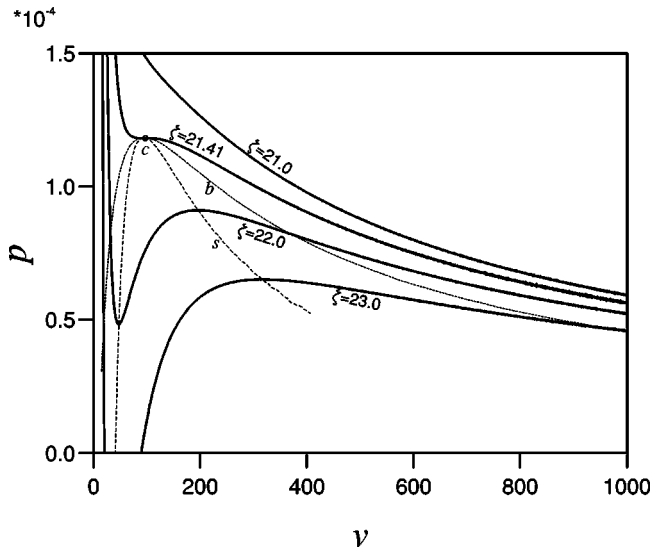


FIG. 2. The $pV$ diagram showing van der Waals loops for various values of $\zeta$. The pressure $p$ has units of $3Z^2e^2/32\pi^2\epsilon a^4$. The binodal is marked $b$, the spinodal $s$, and the critical point $c$.

this translates into a van der Waals loop in the $pV$ diagram, indicating coexistence between a dense and a rarefied phase.

At constant $v$, it is observed that

$$f(C|Z|,Ca)=Cf(|Z|,a), \tag{6}$$

where $C$ is a constant. This is made plausible by the consideration of the expressions for $f$. The electrostatic terms $f_{pair}$ and $f_{self}$ both consist largely (though not entirely) of a function of $\kappa a$ multiplied by $Z^2/a$. Equation (5) shows that the parameter $\kappa a$ can be expressed, at constant $v$, as a function of $|Z|/a$. Meanwhile, $\Delta f_0$ is equal to a constant (at constant $v$) multiplied by $|Z|$. The fact that Eq. (6) appears to hold, according to our numerical results, suggests that all the contributions to the electrostatic free energy, written in units of $Z^2/a$, could be expressed (at constant $v$) as functions of $\kappa a$, even if this is not apparent from the form in which they are written. The relation makes the various components of $f$, if they are expressed in units of $Z^2e^2/8\pi\epsilon a$, dependent only on a parameter $\zeta=|Z|/10^9a$, and not on $Z$ and $a$ separately. The dependence on $|Z|$ and $a$ reduces to $\zeta$ dependence.

Figures 1 and 2 show the free energy $f$ per macroion and pressure $p=-\partial f/\partial v$, respectively, as functions of $v$, for various values of $\zeta$, given in units of $\mathrm{nm}^{-1}$. These graphs show evidence of phase coexistence: the binodal is marked $b$, the spinodal $s$, and the critical point $c$. The value of $\zeta$ at the critical point is $\zeta_c=21.41\ \mathrm{nm}^{-1}$; at each value of the macroion radius $a$, phase coexistence between a dense and a rarefied region emerges as the charge is increased above a critical value $Z_c=\zeta_c a$. The occurrence or nonoccurrence of phase separation at a given $Z$ and $a$ is governed by the value of $\zeta$. This conclusion is similar, although not identical, to that of Ise *et al.* [28], who suggested that the macroion surface charge density (proportional to $Z/a^2$) is the important factor.

### III. THE SQUARE GRADIENT APPROXIMATION

We now outline a method by which the free energy cost of forming a surface between two phases of a fluid can be calculated, if we know the characteristics of the fluid and the phases, using implicitly the ideas of classical density functional theory with the square gradient approximation [29,30]. Along with more sophisticated density functional theories [31], this has often been applied to molecular systems, and recently it has been applied by Brader and Evans [32] to a colloid-polymer mixture.

Consider a system containing two phases $\alpha$ and $\beta$ (with volumes $V^\alpha$ and $V^\beta$ and free energy densities $\rho_F^\alpha$ and $\rho_F^\beta$) separated by an interface. The system has total Helmholtz free energy $F$; we define the excess free energy $F^x$ as the difference between the free energy of a system and the value which the free energy would take if the system contained the two homogeneous phases and an idealized, infinitesimally thin boundary with no free energy of its own:

$$F^x=F-\rho_F^\alpha V^\alpha-\rho_F^\beta V^\beta. \tag{7}$$

If we use the equimolar dividing surface, then $F^x=\sigma A_s$, where $A_s$ is the area of the surface. The surface tension $\sigma$ can be found by

$$\sigma=\int_{-\infty}^{\infty}\rho_F^x(z)dz, \tag{8}$$

where $\rho_F^x(z)$ is the density in space of the excess Helmholtz free energy and $z$ is the distance measured perpendicular to the surface, which is considered here to be planar and to be homogeneous except in the $z$ direction.

The idea of density functional theory, as applied to this problem, is to choose a physically plausible form for the excess free energy density $\rho_F^x[n(z)]$ as a functional of the particle density profile $n(z)$ and then to minimize the total excess free energy density $F^x=A_s\int_{-\infty}^{\infty}\rho_F^x[n(z)]dz$, for given $\alpha$ and $\beta$, with respect to $n(z)$ to find the physical particle density profile $n_{phys}(z)$ between phases $\alpha$ and $\beta$. The physi-

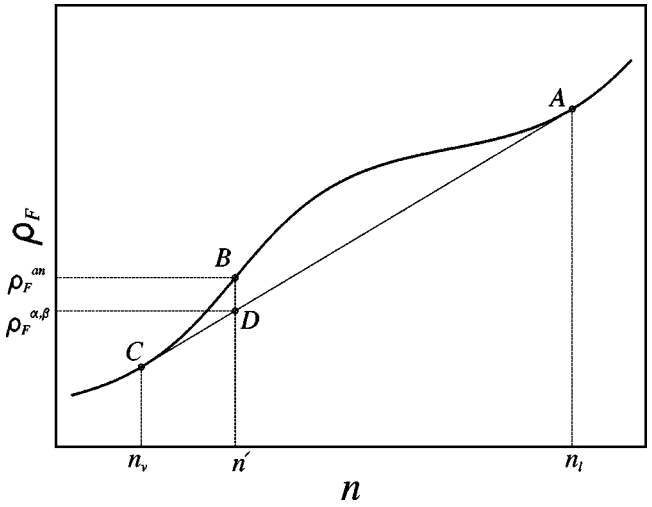


FIG. 3. Illustration of generic free energy density $\rho_F$ against particle density $n$, illustrating components of the free energy density in the local density and square gradient approximations. The location of the equilibrium liquid is marked *A*, and that of the equilibrium vapor *C*. *B* indicates the metastable fluid (with free energy calculated by analytic extension into the metastable region of the free energy curve in the stable regions), while *D* denotes the phase separated state (ignoring the effects of the interface in the calculation of the free energy).

cal excess free energy density will then be $\rho_F^x[n_{phys}(z)]$. The accuracy of the results depends, of course, on a reasonable expression for the excess free energy density having been chosen.

Here, the main aim is to calculate the surface tension rather than the details of the interfacial structure. A first approximation for $\rho_F^x(z)$, known as the local density or point-thermodynamic approximation, is that the free energy density $\rho_F(z)$ at a point in the interfacial region where the particle density is $n'$ is the same as that in a homogeneous phase of density $n'$. This amounts to assuming that local inhomogeneities have no effect on the free energy, which is therefore a function only of the local density. It leads to

$$\rho_F^x(z)=\rho_F^{an}(z)-\rho_F^{\alpha,\beta}, \tag{9}$$

where $\rho_F^{an}(z)$ is the free energy density calculated by analytic extension into the metastable region of the free energy curve in the stable regions (a function only of the local density), and $\rho_F^{\alpha,\beta}$ is the free energy density resulting from the mixture of homogeneous states $\alpha$ and $\beta$, ignoring the effects of the interface. Figure 3 illustrates the situation on the $\rho_F(n)$ diagram: $\rho_F^{an}$ is on the upward bulge, while $\rho_F^{\alpha,\beta}$ is on the tie line. Unfortunately, minimization of $F^x$ would produce a step function interface (for which the local density approximation gives zero excess free energy, since the width of the interface can be taken to zero while $\rho_F^x$ remains finite despite the fact that $|\partial n/\partial z|\to\infty$, as $\rho_F^x$ does not depend on the gradient). The square gradient approximation adds a term proportional to the square of the density gradient:

$$\rho_F^x(z)=\rho_F^{an}(z)-\rho_F^{\alpha,\beta}+C(n)\left(\frac{\partial n}{\partial z}\right)^2. \tag{10}$$

The extra term is to be regarded as the next in an expansion in terms of the derivatives of the density; Eq. (10) is thus strictly valid only for small gradients. The parameter $C$ should be independent of $\partial n/\partial z$ and higher derivatives.

In this approximation, the total free energy density $\rho_F(z)=\rho_F^x(z)+\rho_F^{\alpha,\beta}$ is given by

$$\rho_F(z)=\rho_F^{an}(z)+C(n)\left(\frac{\partial n}{\partial z}\right)^2. \tag{11}$$

Consequently, if $\rho_F(z)$ and $\rho_F^{an}(z)$ can be calculated, we can find $C(n)$ using

$$C(n)=\frac{\rho_F(n)-\rho_F^{an}(n)}{(\partial n/\partial z)^2}. \tag{12}$$

From the Euler-Lagrange equation that minimizes the integral in Eq. (8), where $\rho_F^x(z)$ is given by Eq. (10), we find [30] that

$$\sigma=2\int_{n^\alpha}^{n^\beta}[C(n)(\rho_F^{an}-\rho_F^{\alpha,\beta})]^{1/2}dn. \tag{13}$$

The value of Eq. (13) is that it permits calculation of the surface tension without explicit calculation or consideration of the particle density profile, or even of the density gradient, in the interface [30]. All we need is the coefficient $C(n)$ in the gradient expansion (10).

## IV. THE SQUARE GRADIENT APPROXIMATION APPLIED TO A COLLOIDAL SUSPENSION

In order to calculate the surface tension in a colloidal suspension, we first calculate $C(n)$ at different densities using Eq. (12). At each density $n'$, this requires the calculation of $\rho_F(n')$ and $\rho_F^{an}(n')$. The analytic free energy density $\rho_F^{an}$ is simply the free energy density in a homogeneous phase of particle density $n'$; therefore, it can be evaluated using Eqs. (1) and (2). The procedure for the evaluation of the total free energy $\rho_F$ is more complicated: Eqs. (1) and (2) must be applied in a modified way.

The results produced by these equations depend both on the microion density through the parameter $\kappa a$ (and hence on the macroion density because of the requirement for charge neutrality) and on the macroion separations $S_{mn}$. In the calculation of $\rho_F^{an}$, we approximate the macroion distribution by the simple cubic structure illustrated in the cross section in Fig. 4, and the separations between nearest neighbors, next nearest neighbors, and so on can easily be related to $\kappa a$ using Eq. (5). All macroions are regarded as equivalent, in the sense that the macroion density is a constant throughout the region. The procedure for calculating the electrostatic free energy per macroion is to choose one macroion (marked $m$) and sum over the contributions from its neighbors. Every macroion in the phase can then be regarded as equivalent to this ''test'' macroion.

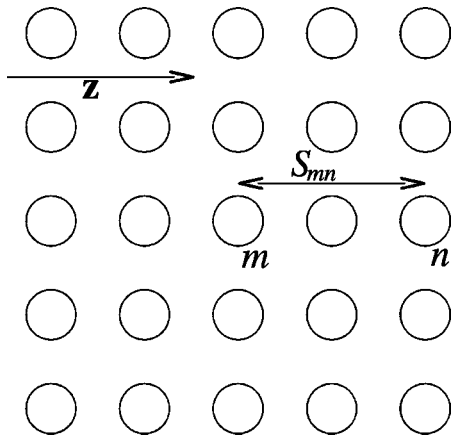


FIG. 4. Schematic of the macroion configuration used in the calculation of the electrostatic free energy density $\rho_F^{an}$ in a homogeneous phase.

For the inhomogeneous system, we consider the lattice shown in the cross section in Fig. 5, with the particle separation varying only in the direction notated as **z**, where **z** is to be interpreted as perpendicular to the surface. This is not intended to be a realistic representation of the interface: it is simply a device to enable us to evaluate the effect of a density gradient on the free energy of the test macroion *m*. The macroion separations are determined by considering each macroion *n* to lie at the center of a cuboidal cell, and associating a density $n_n=1/V_n$ with the macroion, where $V_n$ is the volume of the cell. Let the lengths of those sides of cell *n* that lie parallel to **z** be equal to $s_n$. Other sides of the cell have length $s_m$, where $s_m$ is the side length of the cubic cell around the test macroion *m*. The density at *n* can then be expressed as

$$n_n=\frac{1}{s_m^2 s_n}. \tag{14}$$

The density gradient enters the model as a constant *K*. This does not mean that the density gradient is constant throughout the interface, only that it is possible to define a density gradient that is valid in the vicinity of macroion *m*. The density as a function of distance *z* perpendicular to the interface is thus given by

$$n(z)=n_n+K(z-z_n), \tag{15}$$

where $z_n$ is the value of *z* at some macroion *n*. This density has a physical meaning only at the points occupied by the macroions, and we write

$$n_q=n_n+K(z_q-z_n), \tag{16}$$

where $z_q$ is the *z* coordinate of macroion *q*. Recalling that $n_q=1/(s_m^2 s_q)$, we rewrite Eq. (16) to give

$$n_n+K(z_q-z_n)-\frac{1}{s_m^2 s_q}=0. \tag{17}$$

If *q* and *n* are nearest neighbors in the *z* direction, their separation can be found using Eq. (17). There are two possible cases here. If $q=n+1$, that is $z_q>z_n$, corresponding to $n_q>n_n$ for $K>0$, we have $z_{n+1}-z_n=(s_n+s_{n+1})/2$, which leads to $s_{n+1}=2(z_{n+1}-z_n)-s_n$. Then Eq. (17) is transformed into

$$n_n+Kz_{n,n+1}-\frac{1}{s_m^2(2z_{n,n+1}-s_n)}=0, \tag{18}$$

where $z_{n,n+1}=z_{n+1}-z_n$. This leads on to a quadratic equation for $z_{n,n+1}$ in terms of the densities and the gradient:

$$z_{n,n+1}^2+\left(\frac{n_n}{K}-\frac{n_m^{2/3}}{2n_n}\right)z_{n,n+1}-\frac{n_m^{2/3}}{K}=0. \tag{19}$$

Here, we have used Eq. (14) to find $s_m=1/n_m^{1/3}$ and $s_n=n_m^{2/3}/n_n$. The physically significant solution of Eq. (19) is

$$z_{n,n+1}=\frac{1}{2}\left\{\frac{n_m^{2/3}}{2n_n}-\frac{n_n}{K}+\sqrt{\left(\frac{n_m^{2/3}}{2n_n}-\frac{n_n}{K}\right)^2+\frac{4n_m^{2/3}}{K}}\right\}. \tag{20}$$

The second case is $q=n-1$, that is $z_q<z_n$, which corresponds to $n_q<n_n$ for $K>0$. Then $z_{n,n-1}=-(s_n+s_{n-1})/2$ and $s_{n-1}=-2z_{n,n-1}-s_n$. The quadratic equation in $z_{n,n-1}$ is

$$z_{n,n-1}^2+\left(\frac{n_n}{K}+\frac{n_m^{2/3}}{2n_n}\right)z_{n,n-1}+\frac{n_m^{2/3}}{K}=0, \tag{21}$$

the physically significant solution of which is

$$z_{n,n-1}=-\frac{1}{2}\left\{\frac{n_m^{2/3}}{2n_n}+\frac{n_n}{K}-\sqrt{\left(\frac{n_m^{2/3}}{2n_n}+\frac{n_n}{K}\right)^2-\frac{4n_m^{2/3}}{K}}\right\}. \tag{22}$$

We can calculate the macroion separations that satisfy Eqs. (14) and (16) by starting from the ''test'' macroion *m* and moving outward, repeatedly applying Eq. (20) or Eq. (22) depending on the direction in which we are traveling. This allows us to find macroion separations $S_{mn}$ for the in-

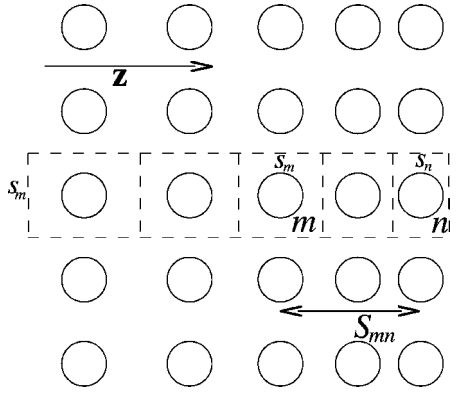


FIG. 5. Schematic of the macroion configuration used in the calculation of the electrostatic free energy density $\rho_F$ of a system with a density gradient. Dashed lines indicate the boundaries of the cells around some of the macroions.

homogeneous system, and these separations can be used in Eqs. (1) and (2), which involve sums over macroions $n$, to estimate the electrostatic free energy per macroion in an inhomogeneous system. The local microion density, which is required for the calculation of $\kappa a$, is assumed to take the same value as it would in a homogeneous system of the same macroion density. One consequence of this assumption is that the only change that the inhomogeneous system requires in the calculation of $f_{el}$ is in the macroion separations $S_{mn}$. As the density gradients are required to be small for the square gradient approximation to be valid, we take the ideal gas contribution $\Delta f_0$ to the free energy to have the same value in the inhomogeneous system as in a homogeneous system of the same macroion density.

The difference that appears in the numerator of Eq. (12) for $C$ can be expressed as a difference in electrostatic free energy contributions:

$$\rho_F(n)-\rho_F^{an}(n)=n[f_{el}(n,K)-f_{el}^{an}(n)], \tag{23}$$

where $f_{el}$ is the electrostatic free energy per macroion in the inhomogeneous system, calculated using Eqs. (1) and (2) as detailed above, and $f_{el}^{an}$ is the electrostatic free energy per macroion in a homogeneous system at the same density. According to the square gradient approximation, the calculated value of $C$ should be a function of the density $n$, but should not depend on the density gradient $\partial n/\partial z$ at a given value of $n$. Of course, this is only true for small $\partial n/\partial z$, as the square gradient approximation is not expected to be valid in a system with a large density gradient.

Having calculated $C$ numerically as a function of density, we can insert it into Eq. (13); the integral can then be performed numerically in order to evaluate the surface tension. This procedure also requires the calculation of $\rho_F^{\alpha,\beta}$, which can be found using the geometry of Fig. 3. Since the state on the bulge and the state on the tie line have the same macroion density, the ideal gas contributions to the free energy of the two states can be regarded as equal. Therefore,

$$\rho_F^{an}-\rho_F^{\alpha,\beta}=n\left[f_{el}^{an}(n)-\left(\frac{n^\beta-n}{n^\beta-n^\alpha}\right)f_{el}^{\alpha}-\left(\frac{n-n^\alpha}{n^\beta-n^\alpha}\right)f_{el}^{\beta}\right], \tag{24}$$

where $f_{el}^{\alpha}$ and $f_{el}^{\beta}$ are the electrostatic free energies per macroion in homogeneous systems of densities $n^\alpha$ and $n^\beta$.

## V. RESULTS FOR THE SURFACE TENSION

We find that the following relation holds for the surface tensions calculated under conditions of zero added salt:

$$\sigma(C|Z|,Ca)=\frac{1}{C}\sigma(|Z|,a), \tag{25}$$

where $C$ is an arbitrary constant. This means that $\sigma$, if expressed in units proportional to $|Z|/a^2$, depends only on the ratio $\zeta=|Z|/10^9a$, and not on $|Z|$ or $a$ individually. Figure 6 shows the calculated surface tension $\sigma$, as a function of volume fraction $\eta$, for a planar interface between the metastable vapor and a phase whose density is equal to that of the equilibrium liquid. The surface tension is expressed in units of $|Z|k_BT/1000a^2$. The domain of the calculations spans the metastable region between the binodal (low $\eta$) and the spinodal (high $\eta$); the surface tension of the interface between the liquid and the equilibrium vapor is at the binodal end of the lines. Because of Eq. (6), the end points of the lines depend only on $\zeta$.

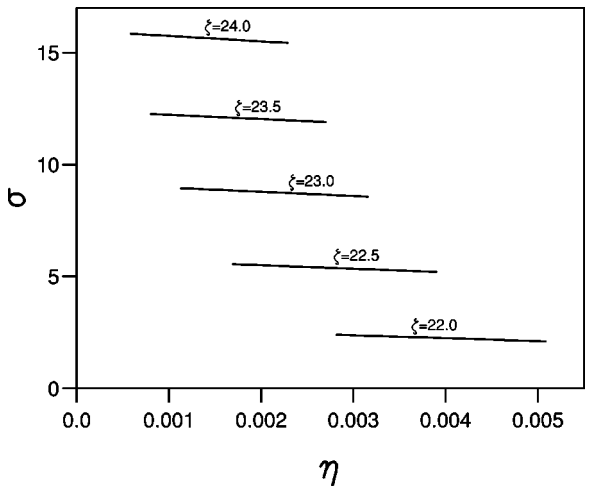


FIG. 6. Surface tension $\sigma$, expressed in units of $|Z|k_BT/1000a^2$, as a function of the volume fraction $\eta$ of the metastable vapor, for various values of $\zeta$ under conditions of zero added salt. The range of values of $\eta$ spans the binodal-spinodal range.

The dependence of $\sigma$ on $\eta$ is weak; the vapor is always much less dense than the liquid, so that small changes in the vapor density have little effect on the difference in density between the two phases, and therefore little effect on the nature of the interface. Figure 6 makes it clear that, at fixed colloid radius, the surface tension (expressed in these units) increases with charge $Z$, and therefore diminishes as the critical point is approached, and that $\sigma$ increases with decreasing macroion radius at fixed charge.

If the macroions have a radius of 50 nm, the actual values of the surface tension are of the order of $10^{-5}$ J m$^{-2}$, which is several orders of magnitude smaller than the surface tensions encountered in molecular fluids ($\sim 10^{-2}$ J m$^{-2}$), but closer to, although slightly larger than, figures measured and calculated for colloid-polymer mixtures [32,33] ($\sim 10^{-6}$–$10^{-5}$ J m$^{-2}$). Experimental and theoretical results [34] for solid-liquid interfaces in hard sphere systems suggest a figure of around $10^{-7}$ J m$^{-2}$ for hard spheres of diameter 100 nm. Larsen and Grier [6] used their observations of metastable colloidal crystallites to estimate a lower limit of $\sim 10^{-8}$ J m$^{-2}$ for charged colloidal particles of radius 326 nm. Our results for $\zeta=22.0$ nm$^{-1}$ suggest a figure of around $5\times 10^{-7}$ J m$^{-2}$ for macroions of this radius, so the Larsen and Grier experiments may have been undertaken very close to the critical point ($\zeta<22$ nm$^{-1}$).

## VI. HOMOGENEOUS NUCLEATION THEORY

### A. Introduction

In the remainder of the paper, we investigate phase metastability and nucleation in a charged colloidal suspension.

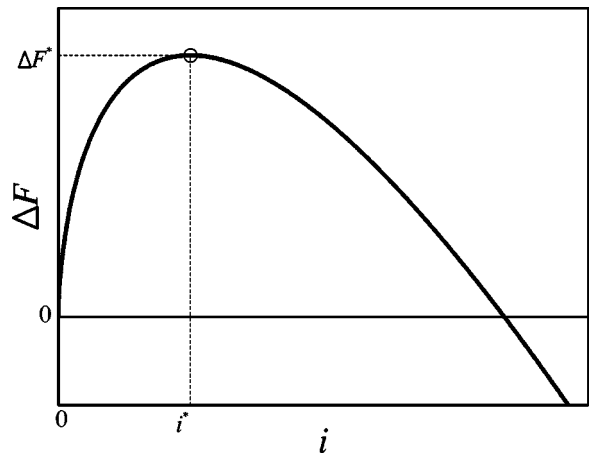


FIG. 7. Illustration of the dependence on the cluster size $i$ of the free energy cost $\Delta F$ of forming a generic liquid cluster from the metastable vapor.

First, we shall introduce the classical theory of homogeneous nucleation. Consider a small liquidlike cluster containing $i$ particles, surrounded by its vapor. We wish to consider the work $\Delta W$ required to form such a cluster from the vapor. In a system whose constraints (constant temperature and volume, and no exchange of matter with the surroundings) are such as to make the Helmholtz free energy $F$ a minimum at equilibrium, the work $\Delta W$ required to cause a reversible process to happen is equal to the change $\Delta F$ in the Helmholtz free energy during the process. With a view to applying the results to the colloidal system discussed in the previous sections, we shall consider nucleation under these external constraints, and so $\Delta W = \Delta F$. This makes the assumption that the states before and after the formation of the cluster can be joined by a reversible path.

We make the assumptions of classical nucleation theory: that is, the cluster can be described as a very small spherical droplet of liquid of radius $R$, which behaves in the same way as a macroscopic spherical drop in the sense that it has a well-defined surface whose area, because of the geometry of the sphere, is proportional to $i^{2/3}$. The surface tension $\sigma$ and density $n_l$ are regarded as having the same values as they would in a macroscopic quantity of liquid under the same conditions. If the cluster is sufficiently small that its formation from the vapor produces a negligible change in the density of the vapor, the free energy cost of forming the cluster from the vapor can be expressed as

$$\Delta F = \Delta f_b i + f_s i^{2/3}, \tag{26}$$

where $\Delta f_b$ is the free energy cost of transferring one particle from the vapor to the liquid phase, and $f_s$ is a parameter proportional to the free energy cost of creating a unit area of the surface. $f_s$ is positive, while, if the vapor is metastable, $\Delta f_b$ will be negative.

The shape of $\Delta F(i)$ is shown in Fig. 7; it possesses a peak at a critical cluster size $i^*$. Clusters larger than $i^*$ will tend to grow, but a cluster can only reach this size by means of random fluctuations: clusters smaller than $i^*$ are unstable with respect to the vapor. The formation probability of a critical cluster is proportional to the exponential of the negative of the work of formation $\Delta F^*$ of the critical cluster, and since a cluster that exceeds the critical size will tend to grow into a macroscopic droplet, we consider the probability of formation of a droplet also to be proportional to this. The Becker-Döring equations relate the nucleation rate $J$ (the rate of formation of droplets) to the formation probability [35], giving, to a good approximation,

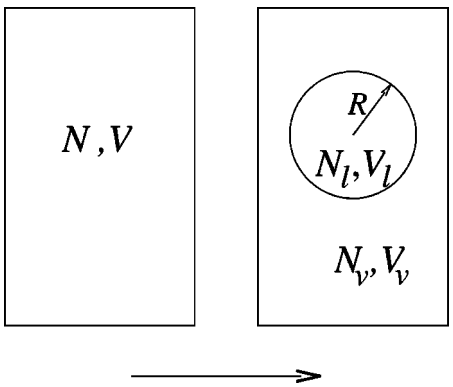


FIG. 8. Schematic of the process of formation of a liquid droplet of radius $R$, volume $V_l$, and density $N_l/V_l$ from a metastable vapor of volume $V$ and density $N/V$.

$$J = J_0 \exp(-\Delta F^*/k_B T), \tag{27}$$

where the prefactor $J_0$ emerges from a detailed consideration of the condensation rate of monomers on to a cluster and their evaporation rate from a cluster. $J_0$ is only weakly dependent on the cluster size, for a given substance under given conditions.

### B. The free energy of formation of a liquid cluster: Classical theory

Now we wish to derive the Helmholtz free energy cost of forming a liquid cluster from the vapor, in order to justify Eq. (26). Figure 8 illustrates schematically the process of formation of an arbitrary droplet or cluster (not necessarily the critical cluster). The initial state consists of a homogeneous metastable vapor of $N$ particles in volume $V$. The final state comprises a spherical liquid cluster of radius $R$ and volume $V_l$, containing $N_l = i$ particles at constant density $i/V_l$, and a vapor of volume $V_v$, containing $N_v$ particles at constant density $n_v = N_v/V_v$. This is the Gibbsian view of the structure of a cluster. The temperature $T$, the total number of particles $N$, and the total volume $V$ are held constant throughout the process. Using the Euler relation of thermodynamics and the definition $F = U - TS$, the free energy $F_h$ of the initial homogeneous state can be written as

$$F_h = -p_h V + \mu_h N, \tag{28}$$

where $p_h$ and $\mu_h$ are, respectively, the pressure and chemical potential in the homogeneous metastable vapor. The free energy after the formation of the cluster is $F = F_l + F_v + F_s$, where the bulk free energy of the liquid cluster is $F_l = -p_l V_l + \mu_l N_l$ ($p_l$ is the pressure in the liquid and $\mu_l$ is the

chemical potential), and that of the remaining vapor is $F_v = -p_v V_v + \mu_v N_v$ ($p_v$ and $\mu_v$ are the pressure and chemical potential in the vapor). The free energy $F_s$ of the (theoretically infinitesimally thin) interface is given by

$$F_s = \sigma A_s + \mu_s N_s , \tag{29}$$

where $\sigma$ is the surface tension, $A_s$ is the surface area of the cluster, $\mu_s$ is the chemical potential in the surface, and $N_s$ is the number of particles associated with the surface. The $\sigma A_s$ term has been added to the energy, and therefore to the Helmholtz free energy, in place of a $-pV$ term. The excess value $F^x$ of the free energy after the cluster has formed is $F_s$. If we choose the interface to correspond to the equimolar dividing surface (which is defined by $N_l + N_v = N$), the excess number of particles $N_s$ is zero and $F_s = \sigma A_s$. This allows the parameter $f_s$, which was introduced in Eq. (26), to be expressed as

$$f_s = (36\pi)^{1/3} \frac{\sigma}{n_l^{2/3}}. \tag{30}$$

Here, of course, we have made the classical assumption that the surface tension is independent of the size of the cluster.

Since $d(\Delta F) = 0$ at $i = i^*$, the critical cluster is in equilibrium with its vapor. This is an unstable equilibrium: the system is unstable against arbitrarily small changes in the size of the cluster. We now consider the chemical potential when the cluster is at the critical size. Using the facts that $V_l + V_v = V$ and $N_l + N_v = N$, we can write the total free energy of a system containing an arbitrary cluster as

$$F = -(p_l - p_v)V_l + (\mu_l - \mu_v)N_l - p_v V + \mu_v N + \sigma A_s . \tag{31}$$

Requiring the unstable equilibrium condition $\partial F / \partial N_l = 0$ to hold, we find that the critical cluster corresponds to the equality of the chemical potentials: $\mu_l^* = \mu_v^*$. (However, the pressures inside and outside the droplet are not equal.)

Subtracting Eq. (28) from Eq. (31), the free energy cost of forming an arbitrary spherical droplet can be expressed as

$$\Delta F = -(p_l - p_v)V_l + (\mu_l - \mu_v)N_l - (p_v - p_h)V + (\mu_v - \mu_h)N + \sigma A_s . \tag{32}$$

The metastable vapor can reasonably be treated as an ideal gas, both before and after the formation of the cluster. Thus we can use the characteristics of the ideal gas to write

$$\mu_v - \mu_h = k_B T \ln\left(\frac{p_v}{p_h}\right) = k_B T \ln\left(1 + \frac{p_v - p_h}{p_h}\right). \tag{33}$$

Provided the cluster is small enough that the perturbations to the vapor due to its formation are small (that is, $p_v \approx p_h$), we can take only the first term in the expansion of $\ln(1+x)$ in powers of $x$, to give

$$\mu_v - \mu_h \approx k_B T \left(\frac{p_v - p_h}{p_h}\right) = (p_v - p_h)\frac{V}{N}, \tag{34}$$

where the second step follows from the ideal gas equation of state. Thus, the third and fourth terms of Eq. (32) cancel one another, and we are left with

$$\Delta F = -(p_l - p_v)V_l + (\mu_l - \mu_v)N_l + \sigma A_s . \tag{35}$$

The pressure $p_l$ and chemical potential $\mu_l$ of the liquid cluster will not have the same values as the pressure and chemical potential in the bulk equilibrium liquid (the liquid that would eventually appear in the final, mixed equilibrium state), which we will denote by $p_l^{\mathrm{eq}}$ and $\mu_l^{\mathrm{eq}}$, respectively. However, a relation between the two states can be found, in order to eliminate explicit reference to $p_l$ and $\mu_l$. We rewrite Eq. (35) as

$$\Delta F = -(p_l - p_l^{\mathrm{eq}})V_l - (p_l^{\mathrm{eq}} - p_v)V_l + (\mu_l - \mu_v)N_l + \sigma A_s . \tag{36}$$

Thermodynamic integration of the Gibbs-Duhem relation between the bulk equilibrium liquid state and the state of the liquid in the cluster, under the constraints that the temperature $T$ and volume per particle, $v_l$, are held constant (the latter constraint implies that the liquid is incompressible, which is clearly an approximation), leads to the relation

$$p_l - p_l^{\mathrm{eq}} = n_l(\mu_l - \mu_l^{\mathrm{eq}}), \tag{37}$$

where we have used the fact that $v_l = 1/n_l$. Inserting Eq. (37) into Eq. (36), recalling that $n_l V_l = N_l$, and making the assumption that the vapor is perturbed only slightly by the formation of the cluster ($p_v \approx p_h$ and $\mu_v \approx \mu_h$), we find

$$\Delta F = -(p_l^{\mathrm{eq}} - p_h)V_l + (\mu_l^{\mathrm{eq}} - \mu_h)N_l + \sigma A_s . \tag{38}$$

Using the relation $f = \mu - pv$, which results from the definitions of the Helmholtz free energy and the chemical potential, Eq. (38) can be rewritten as

$$\Delta F = [f_l^{\mathrm{eq}} - f_h + p_h(v_l - v_h)]N_l + \sigma A_s . \tag{39}$$

Equation (39), together with Eq. (30), justifies the form for $\Delta F$ given in Eq. (26), with

$$\Delta f_b = f_l^{\mathrm{eq}} - f_h + p_h(v_l - v_h). \tag{40}$$

Figure 9 illustrates on an $f(v)$ diagram the physical plausibility of the above expression for $\Delta f_b$. The line $BD$ is tangential to the analytic free energy curve at $v_h$. The length of line $AE$ is equal to $f_l^{\mathrm{eq}} - f_h$, while the length of $DE$ is equal to $-p_h(v_l - v_h)$, since $p_h$ is $-\partial f / \partial v$ evaluated at $B$. So

$$\Delta f_b = |AE| - |DE|. \tag{41}$$

If an upward bulge, indicating phase coexistence, is present, $\Delta f_b$ will clearly be negative; its magnitude will be the length of the line $AD$. The maximum value of the magnitude of $\Delta f_b$ corresponds to the locally most negative value for $\partial f / \partial v$ (the local maximum of $p$), which is located at the spinodal. As $B$ approaches $C$ (the binodal), $\Delta f_b$ will diminish; when $B$ and $C$ coincide ($v_h = v_v^{\mathrm{eq}}$), the tangents $BD$ and $AC$ will coincide

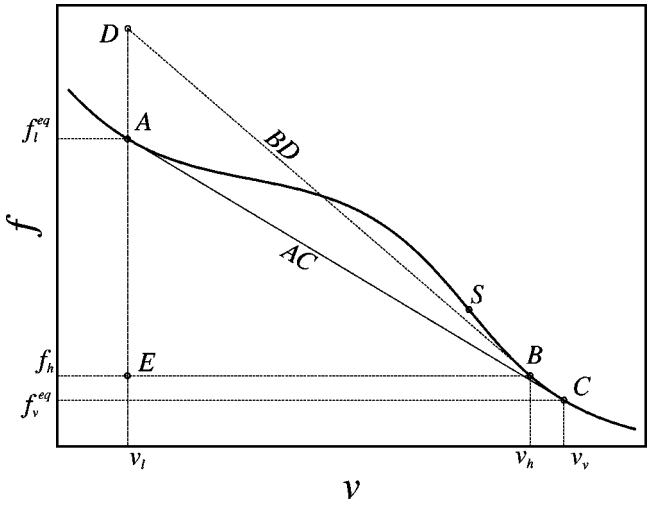


FIG. 9. Illustration of generic free energy $f$ per particle against the volume $v$ per particle, illustrating the qualitative correctness of Eq. (40) for $\Delta f_b$. See text for details.

and $\Delta f_b = 0$. For $v_h > v_v^{\rm eq}$, $\Delta f_b$ is positive, corresponding to a single phase equilibrium state. Finally, $BD$ and $AC$ will coincide also at the critical point, where the analytic free energy curve between $A$ and $C$ becomes a straight line. $\Delta f_b$ is zero here, and becomes negative on the other side of the critical point, where the equilibrium state is a single phase.

Having justified the form of Eq. (26), we can use it to calculate the critical cluster size and work of formation within the classical approximation. The critical cluster is located at the maximum of $\Delta F(i)$, so $(\partial(\Delta F)/\partial i)_{i=i^*} = 0$, which leads to

$$i^* = -\frac{8}{27}\left(\frac{f_s}{\Delta f_b}\right)^3 \tag{42}$$

(recall that $\Delta f_b$ is negative if the vapor is metastable) and therefore

$$\Delta F^* = \frac{4}{27}\frac{f_s^3}{(\Delta f_b)^2} = -\frac{1}{2}\Delta f_b i^*. \tag{43}$$

Inserting Eq. (30) produces

$$i^* = -\frac{32\pi}{3n_l^2}\left(\frac{\sigma}{\Delta f_b}\right)^3 \tag{44}$$

and

$$\Delta F^* = \frac{16\pi}{3n_l^2}\frac{\sigma^3}{(\Delta f_b)^2}. \tag{45}$$

### C. The link with other formulations

Equation (38) is not the most common expression used in the literature to calculate the critical work of formation, and it is important to relate it to the more usual expressions. Consider the form of Eq. (38) when the homogeneous metastable vapor is close to the binodal ($p_h \approx p_v^{\rm eq}$ and $\mu_h \approx \mu_v^{\rm eq}$). Since $p_l^{\rm eq} = p_v^{\rm eq}$ and $\mu_l^{\rm eq} = \mu_v^{\rm eq}$, we have

$$\Delta F = -(p_v^{\rm eq} - p_h)V_l + (\mu_v^{\rm eq} - \mu_h)N_l + \sigma A_s. \tag{46}$$

Of course, both $p_v^{\rm eq} - p_h$ and $\mu_v^{\rm eq} - \mu_h$ go to zero at the binodal. Using the characteristics of an ideal gas, we can rewrite Eq. (46) as

$$\frac{\Delta F}{k_B T} = -(n_v^{\rm eq} - n_h)V_l + \ln\left(\frac{n_v^{\rm eq}}{n_h}\right)N_l + \sigma A_s$$

$$= \left[-\left(\frac{n_v^{\rm eq} - n_h}{n_h}\right)n_h + \ln\left(1 + \frac{n_v^{\rm eq} - n_h}{n_h}\right)n_l\right]V_l + \sigma A_s \tag{47}$$

(where in the second stage we have used the fact that $N_l = n_l V_l$). For small $x$, $\ln(1+x) \approx x$, so near the binodal Eq. (47) becomes

$$\frac{\Delta F}{k_B T} = \left(\frac{n_v^{\rm eq} - n_h}{n_h}\right)(-n_h + n_l)V_l + \sigma A_s; \tag{48}$$

since $n_l \gg n_h$, this leads to the disappearance of the term derived from the $pV$ term in Eq. (46), and

$$\Delta F \approx (\mu_v^{\rm eq} - \mu_h)N_l + \sigma A_s. \tag{49}$$

Expressions of the form (49) for the work of formation are often given in the literature [26,36]. It is important to remember that this expression requires approximations that hold only close to the binodal; thus it can be thermodynamically justified only when the metastable vapor is close to the binodal. Deeper into the coexistence region, it leads to significant, though not catastrophic, errors in calculations for a colloidal system; however, the errors are generally assumed to be insignificant for simple molecular fluids, because $pV$ terms are usually small in such condensed phases.

### D. Modification of classical nucleation theory

Examination of the classical expressions for $i^*$ and $\Delta F^*$ given in Eq. (43) reveals a problem: since both $\Delta f_b$ and $i^*$ are nonzero at the spinodal, $\Delta F^*$ will also be nonzero here, which disagrees with results from density functional theory [37,38]. Intuitively, also, $\Delta F^*$ should go to zero at the spinodal, since the vapor at this point should be unstable against arbitrarily small density fluctuations. It is not surprising that classical nucleation theory is unreliable, since a liquid cluster containing only a small number of particles does not really resemble a macroscopic droplet with a well-defined surface. We shall apply a simple phenomenological correction given by McGraw and Laaksonen [39] and Talanquer [40]. This assumes that, while $i^*$ continues to be expressed by Eq. (42), $\Delta F^*$ contains a correction term that depends only on the temperature:

$$\Delta F^* = -\frac{1}{2}\Delta f_b i^* + D(T). \tag{50}$$

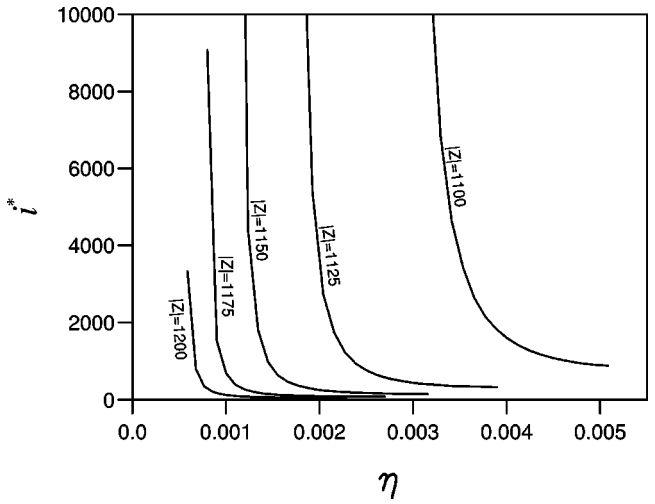


FIG. 10. Critical cluster size $i^*$ as a function of the volume fraction $\eta$ of the metastable vapor, for colloidal particles of radius $a=50$ nm and various charges $Z$, under conditions of zero added salt.

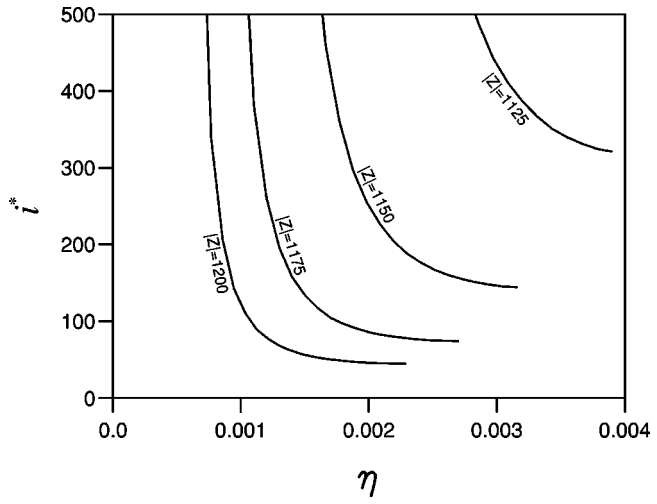


FIG. 11. Critical cluster size $i^*$ as a function of the volume fraction of the metastable vapor, for colloidal particles of radius $a=50$ nm, under conditions of zero added salt. Magnification of Fig. 10.

The correction term $D(T)$ is evaluated by requiring that $\Delta F^*$ vanishes at the spinodal, which gives

$$D(T)=\frac{1}{2}\Delta f_b^{sp} i^{*sp}, \tag{51}$$

where $\Delta f_b^{sp}$ and $i^{*sp}$ are equal to $\Delta f_b$ and the critical cluster size, respectively, evaluated at the spinodal. Thus, the corrected expression for the critical work of formation is

$$\Delta F^*=-\frac{1}{2}(\Delta f_b i^*-\Delta f_b^{sp} i^{*sp}). \tag{52}$$

In the following section we shall use Eq. (52) to calculate some nucleation rates in colloidal systems.

## VII. NUCLEATION IN COLLOIDAL SYSTEMS

When the dependence of the surface tension on the densities of the phases is known, we can calculate the critical size of a liquidlike cluster using equation Eq. (42) and the work of formation of the critical cluster using Eq. (52). Figures 10 and 11 show the variation of the critical size as a function of the colloid volume fraction $\eta$ (and therefore of ''distance'' into the metastable region) for macroions of radius $a=50$ nm and various surface charges. Figure 11 is a magnification of Fig. 10. The critical size approaches infinity at the binodal (the small $\eta$ ends of the lines), and falls rapidly as we move further into the metastable region towards the spinodal (the large $\eta$ ends of the lines). The critical size also increases as the macroion charge decreases towards the critical point ($|Z|=1070$ for $a=50$ nm). This is in line with the results of a recent investigation of the critical size at the approach to the spinodal in molecular systems [41].

Figures 12 and 13 show the barrier to nucleation of the critical cluster for macroions of radius 50 nm (Fig. 13 is a magnification of Fig. 12). The barrier approaches infinity at the binodal, and falls steeply as we move further into the metastable region, reaching zero at the spinodal. Of course, we have modified classical nucleation theory to ensure that the barrier is zero at the spinodal; otherwise it could be of the order $10^2$–$10^3$ $k_BT$.

The calculated homogeneous nucleation rate (density of critical clusters formed per second) is illustrated for macroions of radius 50 nm in Fig. 14. This uses the nucleation rate from Eq. (27), where $\Delta F^*$ is given by Eq. (52) and the prefactor $J_0$ is estimated from classical nucleation theory [42]:

$$J_0=\sqrt{\frac{2\sigma}{\pi m}}\frac{n_h^2}{n_l}. \tag{53}$$

Here, $n_h$ and $n_l$ are the number densities of particles in the homogeneous metastable vapor and the liquid state, respec-

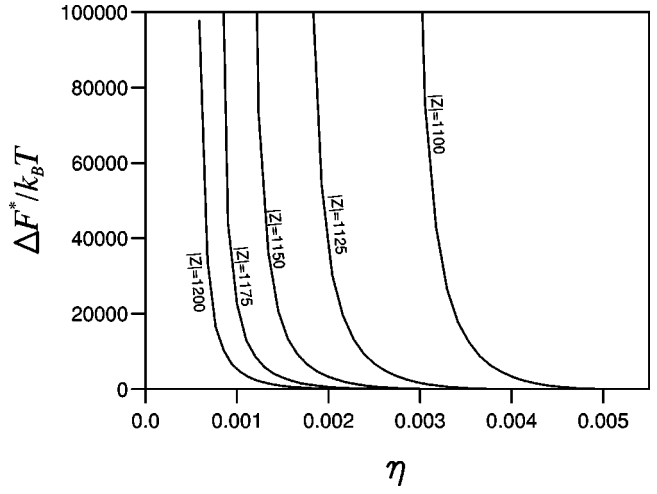


FIG. 12. Nucleation barrier $\Delta F^*$ of the critical cluster as a function of the volume fraction $\eta$ of the metastable vapor, for colloidal particles of radius $a=50$ nm and various charges $Z$, under conditions of zero added salt.

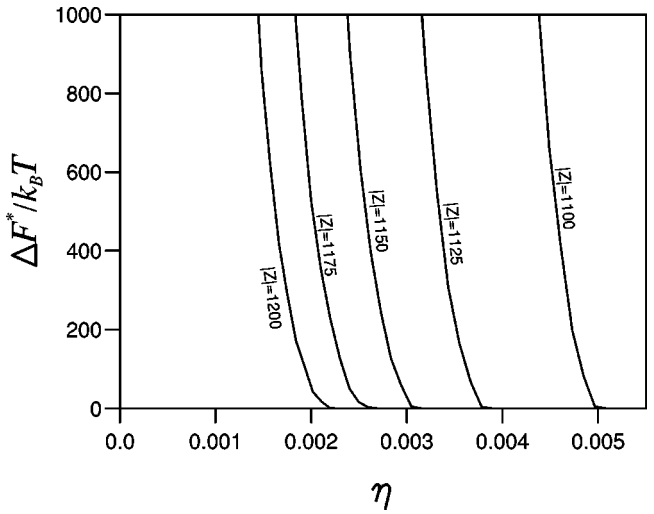


FIG. 13. Nucleation barrier $\Delta F^*$ of the critical cluster as a function of the volume fraction of the metastable vapor, for colloidal particles of radius $a=50$ nm, under conditions of zero added salt. Magnification of Fig. 12.

tively, and the mass $m$ of a particle is calculated by assuming the colloidal particles to have the same density as water. Like the work of formation, the homogeneous nucleation rate depends very steeply on the location within the metastable region of the system prior to phase separation. In most of the metastable region, the nucleation rate is so small that the process would not occur on an observable time scale. It is only in a small region that nucleation rates are in the vicinity of $\ln J=0$, allowing the progress of the nucleation process to be observed as it was (for crystals nucleating from a metastable fluid and voids nucleating from a metastable crystal) by Yoshida *et al.* [8,9].

For $|Z|=1100$ the critical cluster size when $\ln J\approx 0$ is of the order of $10^3$, which is large enough for the assumptions underlying classical nucleation theory to be reasonable. For

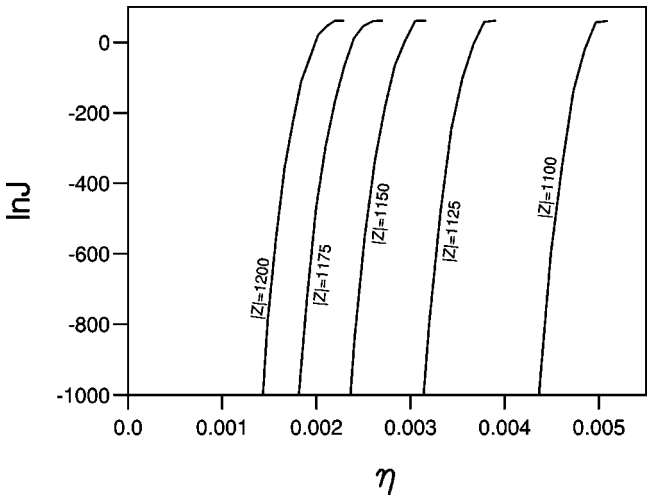


FIG. 14. Natural logarithm $\ln J$ of the nucleation rate as a function of volume fraction, for colloidal particles of radius $a=50$ nm and various charges $Z$, under conditions of zero added salt. $J$ has units of $\mathrm{m}^{-3}\,\mathrm{s}^{-1}$.

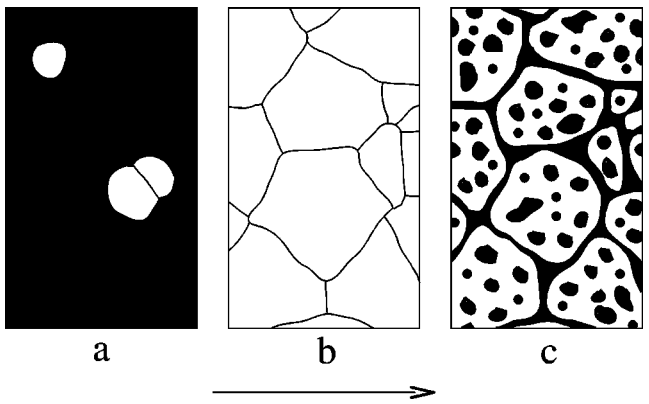


FIG. 15. The Swiss cheese effect discovered by Yoshida *et al.* White represents solidlike (ordered) regions, while black represents liquidlike and gaslike (disordered) regions. A solidlike phase nucleates (a) from the initial liquidlike state on a time scale of seconds to minutes, to produce space-filling crystals (b). Then gaslike regions form within the crystals and at their interfaces (c), on a time scale of minutes to hours.

$|Z|=1200$, this critical cluster size is of the order of 50, and classical nucleation theory begins to appear implausible. If the macroion surface charge were larger than this, there would be no reason to think that an observed homogeneous nucleation process could be described using the classical theory, since it would involve critical clusters too small to be regarded as liquidlike droplets with surfaces.

The upper limit of the nucleation rate would be limited by the rate at which colloidal particles can diffuse, and would not be well described by classical nucleation theory.

## VIII. THE SWISS CHEESE EFFECT

Finally, we shall discuss the Swiss cheese effect [8,9] (see Fig. 15) with reference to nucleation theory. This phenomenon involves the formation of space-filling crystals from an initial disordered (liquidlike) state on a time scale of seconds to minutes, followed by the formation of gaslike regions, on a time scale of minutes to hours, both within the crystals and at the interfaces between them.

We hypothesize that the initial disordered state is metastable with respect to a solidlike state, which is itself metastable with respect to the final phase separated state comprising a solidlike phase of slightly higher density together with a gaslike phase. The initial state lies in a region of the phase diagram where the most thermodynamically favorable single phase is solidlike, and this solidlike phase can nucleate fairly quickly (on a time scale of seconds to minutes): the initial liquidlike phase and the nucleating solidlike phase have similar densities and therefore the surface tension of their interface is small. The fact that the metastable crystallites appear throughout the bulk of the suspension demonstrates that the process of homogeneous nucleation is taking place.

The nucleation of the gaslike regions within and between the metastable crystals is a much slower process, because the large difference in the densities of the two phases leads to a relatively large surface tension, and therefore to a large barrier to nucleation. There is evidence of both homogeneous

(in the interiors of the crystals) and heterogeneous nucleation here: the heterogeneous nucleation takes place at the interfaces between crystals and is the cause of the gaps that form between them. This process happens because particles at the interface are already thermodynamically ''disadvantaged'' by the presence of the interface, and so the additional free energy required to form the surface of a gaslike region is smaller than it is in the bulk. However, the heterogeneous nucleation is not so much more favored that it preempts homogeneous nucleation and prevents it from being observed; if this were the case, the ''cheese'' would have no holes in it.

There is another mechanism that could contribute to the appearance of gaslike regions at the interfaces of the crystals: small bubbles of the gaslike phase, formed by homogeneous nucleation, could diffuse to an interface from the body of a crystal. This process is thermodynamically favorable since it reduces the surface area of the crystal. However, we cannot attribute the formation of the gaslike regions at the interfaces entirely to this mechanism; if homogeneous nucleation occurs in the interior of the crystals, heterogeneous nucleation at the interfaces seems inevitable, since it is by definition a faster process than homogeneous nucleation.

It can be seen from Fig. 14 that the rate of homogeneous nucleation is vanishingly small in most of the metastable region, so that in practice the process would only be observed in a small part of the region. This is not just a feature of colloidal systems: it results from the exponential dependence of the nucleation rate on the work of formation of the critical cluster, and applies also to simple fluids. However, in simple fluids the process of homogeneous nucleation is usually preempted by heterogeneous nucleation (because the roughness on the molecular scale of the surfaces of impurities and of the walls of the container provides highly advantageous sites for heterogeneous nucleation), so that a metastable state is unlikely to endure for long. It was argued at the beginning of this paper that this should not be the case for colloidal systems, and the experimental results of Yoshida *et al*. support this conclusion.

Unless heterogeneous nucleation were much faster than homogeneous nucleation in a particular colloidal suspension, metastable states in most of the metastable region would, to all intents and purposes, be stable: phase separation would not be seen to occur on any experimentally accessible time scale. Thus, consideration of surfaces and nonequilibrium processes would be essential to the study of these systems. Even an exact calculation of the equilibrium phase diagram would be an incomplete description of the phase behavior: only a calculation of the nucleation rates could tell us which phase separated states would be observed in practice. These conclusions are also relevant to computer simulations: in most parts of the metastable region, simulations would have to run for an extremely long time before evidence of phase separation could be detected.

However, the experiments of Yoshida *et al*. suggest a mechanism by which phase separation could occur even if direct homogeneous nucleation were too slow a process to be observable, even if there were no possibility of heterogeneous nucleation at the walls of the container. If the system is in a region of the phase diagram where the most stable state of homogeneous density is solidlike rather than disordered, an initially disordered state will tend to change to the solidlike state, and this will happen much more easily than the phase separation into a dense and a rarefied phase. The competing crystals that result from this first nucleation process will leave interfaces at which heterogeneous nucleation might take place, although in this particular experimental system the process does not appear to be significantly faster than homogeneous nucleation.

## IX. CONCLUSIONS

Our results predict that the Helmholtz free energy of a charged colloidal suspension containing univalent microions and no added salt, expressed in dimensionless units, depends on the ratio of the macroion charge to the macroion radius, and not on the charge or radius separately. This simplifies the description of the phase behavior, and implies that the occurrence or nonoccurrence of phase separation into a dense and a rarefied phase is governed by this ratio.

This paper has presented the first theoretical estimates of surface tension in charged colloidal suspensions, calculated using density functional theory in the square gradient approximation. The calculated values are of a reasonable order of magnitude, and approach zero, as expected, as the critical macroion surface charge is approached. Knowledge of the surface tension allows the characteristics of the critical cluster, and therefore also the rate of homogeneous nucleation, to be calculated, at least within classical nucleation theory. The results emphasize the fact that the homogeneous nucleation rate depends very steeply on the conditions, so that, in large parts of the metastable region, homogeneous nucleation would not be observed on any practical time scale. Physical arguments and experimental evidence suggest that heterogeneous nucleation is not significantly faster than homogeneous nucleation in many colloidal systems; in this case, phase separation might never occur in large parts of the metastable region, and the calculation of nucleation rates would then be as important as equilibrium calculations in the theoretical prediction of phase coexistence.

The Swiss cheese effect observed by Yoshida *et al*. [9] can be explained qualitatively in the context of nucleation theory. The initial formation of competing metastable crystals from a metastable liquidlike phase is evidence of homogeneous nucleation, while the subsequent formation of gaslike regions shows signs of both homogeneous and heterogeneous nucleation. The possibility of heterogeneous nucleation at the boundaries of metastable crystals suggests a mechanism by which phase separated states that are inaccessible by homogeneous nucleation might nonetheless be observed, even in the absence of other heterogeneous nucleation sites.

## ACKNOWLEDGMENT

This research was supported by the U.K. Engineering and Physical Sciences Research Council (EPSRC).

[1] N. Ise, T. Okubo, K. Yamamoto, H. Kawai, T. Hashimoto, M. Fujimura, and Y. Hiragi, J. Am. Chem. Soc. **102**, 7901 (1980).
[2] N. Ise, T. Okubo, M. Sugimura, K. Ito, and H.J. Nolte, J. Chem. Phys. **78**, 536 (1983).
[3] A.K. Arora, B.V.R. Tata, A.K. Sood, and R. Kesavamoorthy, Phys. Rev. Lett. **60**, 2438 (1988).
[4] B.V.R. Tata, M. Rajalakshmi, and A.K. Arora, Phys. Rev. Lett. **69**, 3778 (1992); T. Palberg and M. Würth, *ibid.* **72**, 786 (1994); B.V.R. Tata and A.K. Arora, *ibid.* **72**, 787 (1994).
[5] K. Ito, H. Yoshida, and N. Ise, Science **263**, 66 (1994).
[6] A.E. Larsen and D.G. Grier, Nature (London) **385**, 230 (1997).
[7] B.V.R. Tata, E. Yamahara, P.V. Rajamani, and N. Ise, Phys. Rev. Lett. **78**, 2660 (1997).
[8] H. Yoshida, J. Yamanaka, T. Koga, N. Ise, and T. Hashimoto, Langmuir **14**, 569 (1998).
[9] H. Yoshida, J. Yamanaka, T. Koga, T. Koga, N. Ise, and T. Hashimoto, Langmuir **15**, 2684 (1999).
[10] E.J.W. Verwey and J.Th.G. Overbeek, *Theory of the Stability of Lyophobic Colloids* (Elsevier, New York, 1948).
[11] R. J. Hunter, *Foundations of Colloid Science*, 2nd ed. (Oxford University Press, Oxford, 2001).
[12] I. Sogami and N. Ise, J. Chem. Phys. **81**, 6320 (1984).
[13] R. van Roij, M. Dijkstra, and J.-P. Hansen, Phys. Rev. E **59**, 2010 (1999).
[14] R. van Roij and R. Evans, J. Phys.: Condens. Matter **11**, 10 047 (1999).
[15] P.B. Warren, J. Chem. Phys. **112**, 4683 (2000).
[16] M. Knott and I.J. Ford, Phys. Rev. E **63**, 031403 (2001).
[17] D.Y.C. Chan, P. Linse, and S.N. Petris, Langmuir **17**, 4202 (2001).
[18] L.B. Bhuiyan and C.W. Outhwaite, J. Chem. Phys. **116**, 2650 (2002).
[19] C. Domb, *The Critical Point* (Taylor & Francis, London, 1996).
[20] A. Diehl, M.C. Barbosa, and Y. Levin, Europhys. Lett. **53**, 86 (2001).
[21] V. Reus, L. Belloni, T. Zemb, N. Lutterbach, and H. Versmold, J. Phys. II **7**, 603 (1997).
[22] L. Belloni, J. Phys.: Condens. Matter **12**, R549 (2000).
[23] P. Linse, J. Chem. Phys. **113**, 4359 (2000).
[24] J. Reščič and P. Linse, J. Chem. Phys. **114**, 10131 (2001).
[25] P.G. Debenedetti, *Metastable Liquids* (Princeton University Press, Princeton, NJ, 1997).
[26] D.W. Oxtoby, J. Phys.: Condens. Matter **4**, 7627 (1992).
[27] A.K. Sood, Solid State Phys. **45**, 1 (1991).
[28] N. Ise, T. Konishi, and B.V.R. Tata, Langmuir **15**, 4176 (1999).
[29] J.W. Cahn and J.E. Hilliard, J. Chem. Phys. **28**, 258 (1958).
[30] J.S. Rowlinson and B. Widom, *Molecular Theory of Capillarity* (Clarendon Press, Oxford, 1982).
[31] R. Evans, in *Fundamentals of Inhomogeneous Fluids*, edited by D.Henderson (Dekker, New York, 1992).
[32] J.M. Brader and R. Evans, Europhys. Lett. **49**, 678 (2000).
[33] E.H.A. de Hoog and H.N.W. Lekkerkerker, J. Phys. Chem. B **103**, 5274 (1999).
[34] D.W. Marr and A.P. Gast, Langmuir **10**, 1348 (1994).
[35] F.F. Abraham, *Homogeneous Nucleation Theory* (Academic Press, New York, 1974).
[36] D. Kashchiev, *Nucleation: Basic Theory with Applications* (Butterworth-Heinemann, Oxford, 2000).
[37] J.W. Cahn and J.E. Hilliard, J. Chem. Phys. **31**, 688 (1959).
[38] D.W. Oxtoby and R. Evans, J. Chem. Phys. **89**, 7521 (1988).
[39] R. McGraw and A. Laaksonen, Phys. Rev. Lett. **76**, 2754 (1996).
[40] V. Talanquer, J. Chem. Phys. **106**, 9957 (1997).
[41] M.P. Anisimov, I.N. Shaymordanov, and P.K. Hopke, J. Aerosol Sci. **32**, S17 (2001).
[42] D.W. Oxtoby, in *Fundamentals of Inhomogeneous Fluids* (Ref. [31]).